20

Influence of immersion agents on optical parameters of bio-tissues during laser photothermal therapy of tumor: pilot study

© V.D. Genin[1,2], A.B. Bucharskaya[3], N.A. Navolokin[3], G.S. Terentyuk[3], N.G. Khlebtsov[4], V.V. Tuchin[1,2,5], E.A. Genina[1,2]

[1] Saratov National Research State University n/a N.G. Chernyshevsky,
410012 Saratov, Russia
[2] Tomsk State University,
634050 Tomsk, Russia
[3] Saratov State Medical University n/a V.I. Razumovsky,
410012 Saratov, Russia
[4] Institute of Biochemistry and Physiology of Plants and Microorganisms of the Russian Academy of Sciences, FRC „Saratov Science Center of the RAS“,
410049 Saratov, Russia
[5] Institute for Precision Mechanics and Control Problems of the Russian Academy of Sciences, FRC „Saratov Science Center of the RAS“,
410028 Saratov, Russia

e-mail: versetty2005@yandex.ru

Received December 23, 2021
Revised January 17, 2022
Accepted March 23, 2022

Combined use of an immersion agent with low-intensity laser irradiation for optical clearing of skin before plasmon photothermal therapy (PPTT) procedure is offered. Pilot study results of influence of the immersion agents on optical parameters of skin, subdermal connective tissue and model tumor of rats *in vivo* at hyperthermia during PPTT are presented. Model of alveolar liver cancer — cholangiocarcinoma, transplanted under the skin, was used as a model tumor. For PPTT the gold nanorods with absorption band in the area of diode laser radiation (808 nm) were introduced. Monitoring of light attenuation coefficient change in skin at optical clearing was performed using optical coherent tomography. Measurements of optical parameters of the complete tumor and its layers were performed using spectrometers in a wave length range of 350−2200 nm. Reduction of skin thermal damage during PPTT with preliminary optical clearing using immersion agent (mixture of 70% glycerol water solution and 10% DMSO) and low-intensity laser irradiation at wave length of 808 nm is observed.

Keywords: gold nanorods, IR laser radiation, optical clearing, optical parameters, plasmon photothermal therapy.

DOI: 10.21883/EOS.2022.06.54704.27-22

1. Introduction

Photothermal therapy (PTT), that belongs to treatment methods, based on photothermal conversion under light radiation, attracts more attention due to its increasing potential application in oncology [1–3]. Due to presence of severe side effects of the traditional tumor treatment strategies, such as chemotherapy and X-ray therapy, PTT can eventually become their alternative. Besides, the light irradiation allows to control its time and spatial characteristics during tumor removing. Plasmon resonance nanoparticles with local surface plasmon resonance in a certain spectral band can be used to improve laser radiation selectivity [4–6]. Such nanoparticles, absorbing the radiation with the corresponding wave length, are capable to generate thermal energy in local volume, allowing to reduce the laser radiation dose and lower the damage, inflicting to healthy tissues around the tumor. Gold nanorods (GNR) are successfully used at plasmon resonance photothermal therapy (PPTT) [7–9]. Use of near IR radiation, falling into bio-tissues transparency window of NIR-I (625−975 nm) [10], for excitation of plasmonic resonance gives an advantage compared to other spectral bands, since it is absorbed in a less degree by the main chromoforms: melanin, hemoglobin and water. However, due to light scattering in skin tissues the depth of laser radiation penetration decreases [11].

Significant number of works, dedicated to the optical clearing of skin *in vivo* by introduction of the immersion optical clearing agents (OCA), showed the great potential of such approach for improvement of visualization of hidden heterogeneities and blood vessels [12–15]. Solutions of biocompatible preparations, such as glycerol [16,17], polyethylenglycol [14,18], glucose [15,19] and others combining with dimethyl sulfoxide (DMSO) [20,21], that contributes to epidermis permeability increase, are most frequently used as OCA.

Earlier studies of optical clearing at combined use of OCA and laser radiation with various wave lengths (CO_2-laser and Nd:YAG-laser, operating at wave lengths of 532 and 1064 nm, diode laser, operating at wave length of 980 nm,

and sources of broadband intensive pulse light, operating in the ranges of 650−1200, 525−1200 and 470−1400 nm) and intensity were presented in the works [23,24], where heating of skin surface *in vivo* was used before OCA application. The results of skin study on irradiated sections using the optical coherent tomography (OCT) showed the increase of light penetration depth by 42% [23]. Based on reflection spectra measurement before and after irradiation the improvement of OCA transepidermal penetration by a factor of 8−9 is showed compared to unirradiated skin [24]. Combined use of PPTT for subdermal tumors and optical clearing of skin was first described in the work [25]. This approach can improve the procedure efficiency, particularly in the works [11,26], using computer simulation and experimentally on samples of tissues *ex vivo* and animals *in vivo*, the increase of skin temperature during its irradiation on a wave length of 1064 nm and preliminary clearing was showed.

Study of thermally induced changes of optical properties of tumor tissues at PPTT is important both for evaluation of the required dose of the introduced nanoparticles and laser irradiation, and for development of mathematical models, that can reliably predict the results of PPTT procedure under various conditions, including during optical clearing of surface tissues. Despite the multiple studies of optical parameters of skin, blood and tumors during their heating [27–32], the studies of optical parameters change *in vivo* during heating in the presence of OCA, as well as at PPTT with optical clearing, are next to none.

Thus, the purpose of this work is to study the changes of optical parameters of skin and model tumor through the example of cholangiocarcinoma at PPTT and optical clearing of skin.

Materials and methods

70% water solution of glycerol (Gl) and mixture of 70% glycerol, 10% DMSO and 20% water (Gl@DMSO) were used as OCA. Refraction indices, measured at Abbe refractometer IRF 454B2M (LOMO, Russia), were 1.4400 and 1.4245 on a wave length of 589 nm for Gl and Gl@DMSO respectively.

GNR were synthesized in a laboratory of the Institute of Biochemistry and Physiology of Plants and Microorganisms of the Russian Academy of Sciences. To prevent aggregation the particles were functionalized with thiolated polyethylenglycol (molecular weight of 5000 Da, Nektar, USA). Geometrical sizes of GNR (length of 41 ± 8 nm and diameter of 10 ± 2 nm) were defined as per transmission electron microscope images, observed using electron microscope Libra-120 (Carl Zeiss, Germany). Concentration in suspension was 400 mkg/ml with maximum absorbance (20) on a wave length of 800 nm. High value of GNR suspension absorbance provides sufficient heating of tissues around the tumor [9,32].

11 white laboratory outbreed male rats with a weight of 160−200 g, taken from vivarium of the Common Use Center of SSMU named after V. I. Razumovsky, were used in the experiments.

To get the model tumors the suspension of alveolar liver cancer cells PC-1 (cholangiocarcinoma), taken from a tumor strain bank of the Federal State Budgetary Institution „National Medical Research Center of Oncology named after N.N. Blokhin“ of the Ministry of Health of Russia, was introduced to three rats. Cancer cells were implanted to rats under skin in the scapular area, per 0.5 ml of 25% tumor suspension in Hanks solution.

Before the start of the experiments the animals were anaesthetized using 0.5 mg/kg of „Zoletil 50“ (Virbac, France). Wool on the examined skin sections were removed using single-use safety razor.

In the first series of experiments the influence of various stimuli separately and in combination (single-component OCA−Gl and its combination with laser irradiation Gl@laser, two-component OCA−Gl@DMSO and its combination with laser irradiation Gl@DMSO@laser, as well as laser irradiation without OCA−Laser) on optical parameters of skin was studied. 8 healthy rats were used in the experiment. 2 skin sections of each animal with a size of 1.5×1.5 cm, located on the sides symmetrical about a backbone, that were randomly divided into 5 groups. Before the start of the experiments the OCT image of intact sections was registered in all groups. Control studies included group I: Gl was applied to skin surface, group II: Gl@DMSO was applied to skin surface and group III: skin was subject to laser irradiation at a wave length of 808 nm using fiber laser LS-2-N-808-10000 (Laser Systems, Ltd., Russia) with core diameter of 400 μm and numerical aperture of 0.2. In groups IV and V Gl or Gl@DMSO was applied to skin respectively and the irradiation was performed. Volume of the applied OCA was 1 ml. Radiative power in the groups, subject to laser exposure (III-V), was regulated by operator to maintain the almost equal temperature on animals? skin surface in a range of 40−41°C. The average power was 0.9 ± 0.2 W, while the average temperature on the skin surface was up to 40.7 ± 0.4°C. For each animal the irradiation power was constant for the whole experiment. Temperature monitoring was performed continuously using IR visualizer IRI4010 (IRYSYS, UK). The spectral optical coherent tomograph OCP930SR (Thorlabs, USA) with central radiation wave length of 930 ± 5 nm, spectral width of 100 nm, longitudinal and lateral resolution of 6.2 and 9.6 μm (in air) respectively and scan length of 2 mm was used for skin condition monitoring. Scanning was performed every 2 min. Total monitoring time was 15 min. When using OCA only (groups I and II) the animal was always on OCT stage during the experiment. In the groups with laser irradiation use (groups III−V) the stage with animal was shifted for alternate irradiation and OCT scanning, while laser irradiation was interrupted during OCT scanning (10−20 s).

In the second series of experiments three rats with model tumors were used. When tumors volume reached $\geq 3\,\text{cm}^3$, one hour before the experiment the GNR suspension was introduced with a rate of 0.1 ml/min to two rats in three tumor points. The total volume of the introduced suspension was 1 ml with GNR concentration of 400 mkg/ml. This method of introduction results in the nanoparticles accumulation and maintaining in the tumor [33]. Thus, GNR concentration per tumor volume (about $3\,\text{cm}^3$) was about $133\,\text{mkg/cm}^3$.

Before PPTT procedure the OCA Gl@DMSO with a volume of 1 ml was applied to skin surface above tumor of one of the rats and laser irradiation with power of 1 W for 10 min was performed, while power density on a surface was about $1.2\,\text{W/cm}^2$. Then the laser radiation power was increased to 2 W, and irradiation continued for another 15 min, while power density on a skin surface was $2.3\,\text{W/cm}^2$. Skin surface temperature was registered every 0.5 min. Tumor of the second rat was irradiated without preliminary skin clearing for 15 min with the power density of $2.3\,\text{W/cm}^2$. The third rat was not subject to laser irradiation.

Before irradiation and immediately after, the spectra of diffuse reflection of skin above the tumor were registered suing spectrometers USB4000-Vis-NIR (Ocean Optics, USA) in a spectral band of 420–1000 nm and NIRQuest (Ocean Optics, USA) in a spectral band of 930–2125 nm. Halogen lamp HL-2000 (Ocean Optics, USA) was used as a light source. Optical probe QR400-7-VIS/NIR (Ocean Optics, USA), equipped with six radiating lightguides around single receiving fiber with core diameter of 400 μm and numerical aperture of 0.22 ± 0.02, was used for measurement. The probe was fixed in a cylindrical holder with hole diameter, corresponding to the probe diameter, to provide the distance of 2 mm between the skin and the probe. Thus, the diffusive backscattered radiation was received from the skin area of about $8\,\text{mm}^2$. Before the start of measurements the spectrometers were calibrated using a reflectance standard WS-1-SL (Labsphere, USA).

Then all three rats were put out of the experiment. Layers of tissues after irradiation are schematically presented in fig. 1. Tumors with adjoining bio-tissues were removed and divided into the following layers: skin above the tumor, subdermal layer of the connective tissue, upper tumor part and lower tumor part.

Spectra of complete transmission and diffuse reflection of the samples were measured in a wave lengths range of 350–2200 nm. Spectrophotometer UV-3600 (Shimatzu, Japan) with integrating sphere LISR-3100 (Shimatzu, Japan) was used for spectral measurements. Before the measurements the samples were put between two preparation glasses and fixed without pressure. Samples thickness was measured using electron microscope with accuracy of $\pm 1\,\mu$m in five sample points, after which the results were averaged. Diffuse reflection standard $BaSO_4$ was used for the spectrophotometer calibration.

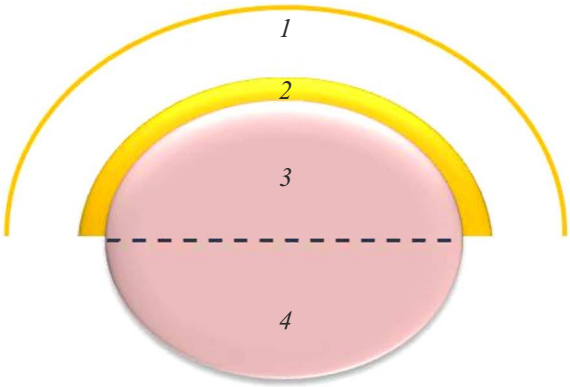

Figure 1. Schematic image of the tumor with the adjoining layers of bio-tissues: skin above the tumor (*1*), subdermal layer of the connective tissue (*2*), upper tumor part (*3*) and lower tumor part (*4*).

Optical light attenuation coefficient was evaluated based on the results of OCT scanning in accordance with the single scattering model [34]:

$$R(z) = A\exp(-\mu_t z) + B, \qquad (1)$$

where $R(z)$ — OCT signal, A — proportionality coefficient, equal to $P_0\alpha(z)$; P_0 — power of optical beam, falling onto the bio-tissue surface, $\alpha(z)$ — bio-tissue reflectivity on a specified depth, defined by the local refraction index and local capability of the bio-tissue to scatter the light backward, $\mu_t = \mu_a + \mu_s$ — coefficient of light attenuation by bio-tissue, μ_a — coefficient of light absorption by bio-tissue. μ_s — coefficient of light scattering by bio-tissue; B — background signal.

Techniques of attenuation coefficient evaluation, when OCT A-scan was approximated with a single exponential dependence and when with two, are presented in fig. 2. Rectangle indicates the area of OCT signal averaging (51 A-scan), that was selected in the area of interest. Typical image of intact skin is presented in fig. 2, *a*, but this approach could be used both to sections after OCA and laser radiation application separately, and to combination of Gl@laser. As a result of Gl@DMSO@laser exposure in the upper and medium skin parts, such changes of OCT signal occurred, that it was impossible to approximate it with single exponential dependence, thus the necessity appeared to use two exponents for the signal approximation (fig. 2, *b*).

For evaluation of μ_t value as an exponential parameter, that shows the best correlation with the curve, the nonlinear least-squares method was used [35,36]. Values of μ_t were defined for each animal, were averaged by groups and normalized by initial value. The standard deviation was calculated for each average value.

Based on the measured spectra of complete transmission and diffuse reflection into the sphere, the absorption coefficient (μ_a) and transport scattering coefficient (μ_s) of the examined tissue samples were calculated. Combined

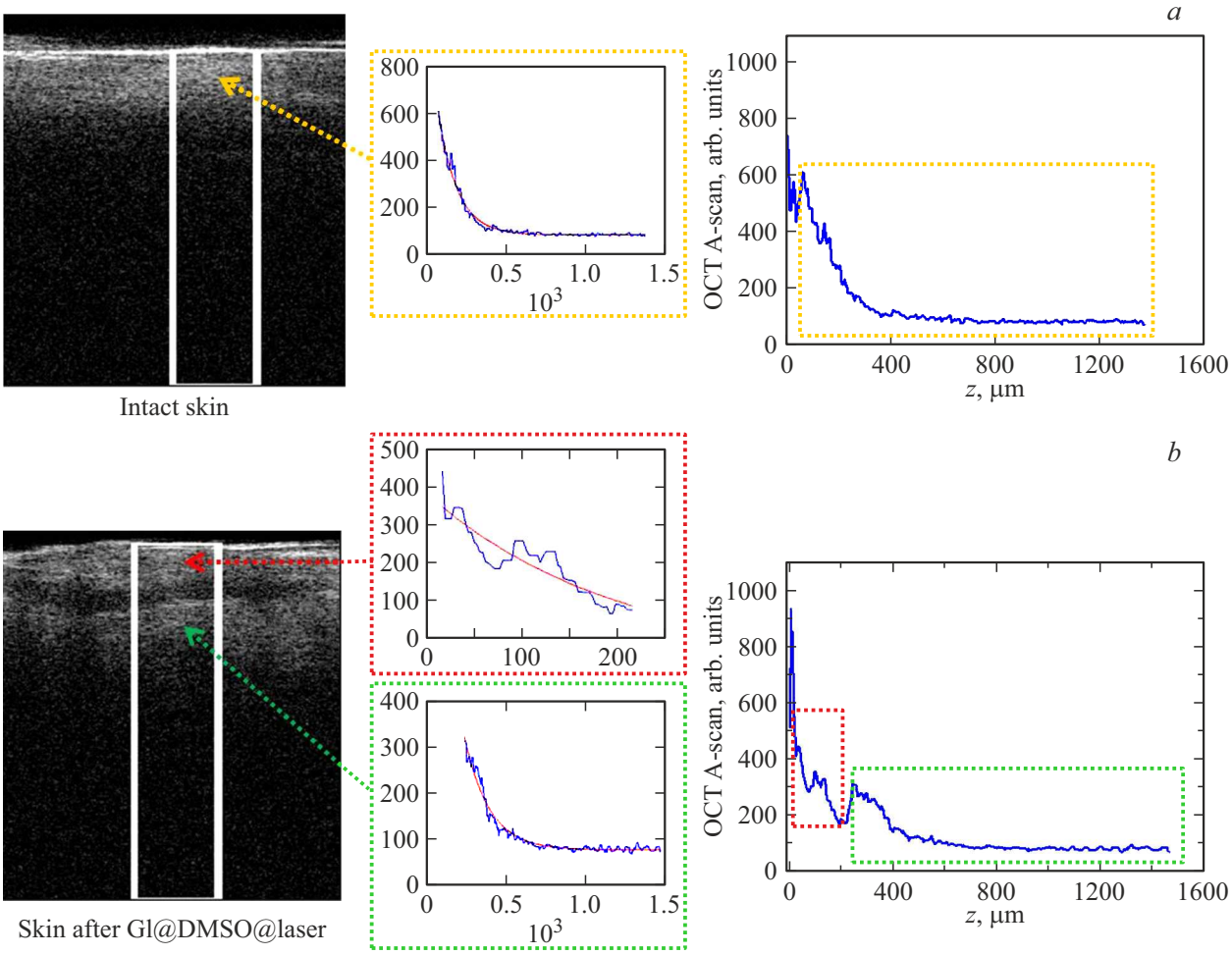

Figure 2. Typical OCT images of a rat skin section *in vivo* (B-scan), averaged A-scan of OCT signal and approximating curves, built using single scattering model (*a*) before the start of exposure (Intact skin) and (*b*) after application of OCA and IR laser irradiation (Gl@DMSO@laser).

approach was used for the experimental results processing and optical parameters determination. At the first stage the measurement data were processed using the method of inverse adding-doubling [37]. Then the accuracy of the observed values of μ_a and μ_s was improved using inverse Monte Carlo method until agreement of the measured and calculated data with the specified accuracy ($< 0.1\%$) [38].

Results and discussion

The results of OCT studies of rats skin *in vivo* under exposure of various stimuli are presented in fig. 3 and 4. It is seen well in fig. 3, *a, b*, that under exposure of Gl and Gl@DMSO the epidermis clears up above all else, the interface between epidermis and skin becomes visible. Efficiency of the optical clearing of a skin is higher when using the solution of Gl@DMSO, than Gl, as evidenced by larger increase of probing depth in the first case. These results are in good agreement with the results, presented in the works [20–22], that show the increase of epidermis permeability when clearing agent DMSO is introduced to solution. Fig. 4, *a* shows decrease of the light attenuation coefficient in skin during optical clearing by 23 ± 9 and $29 \pm 3\%$ for 14 min for Gl and Gl@DMSO respectively. At the same time it is seen, that for Gl@DMSO there is a trend for the further reduction of the attenuation coefficient.

From the results, presented in fig. 3, *b* and 4, *a*, it follows that for combination of Gl exposure and heating the process of glycerol diffusion to skin is accompanied with tissue induration, probably due to tissue dehydration under exposure of hyperosmotic glycerol solution and with temperature increase. During observation the value of μ_t reduces by $18 \pm 10\%$ for 10 min at first, and then increases almost to initial value.

Significant changes compared to other groups were observed during heating of the skin, processed with Gl@DMSO (fig. 3, *d*). It is seen well, that at the same temperature as in other groups, tissue is dissected with edema area formation. At the same time the upper part is indurated during heating, as evidenced by increase of μ_t value by a factor of 3.5 ± 1.3 in average, while the

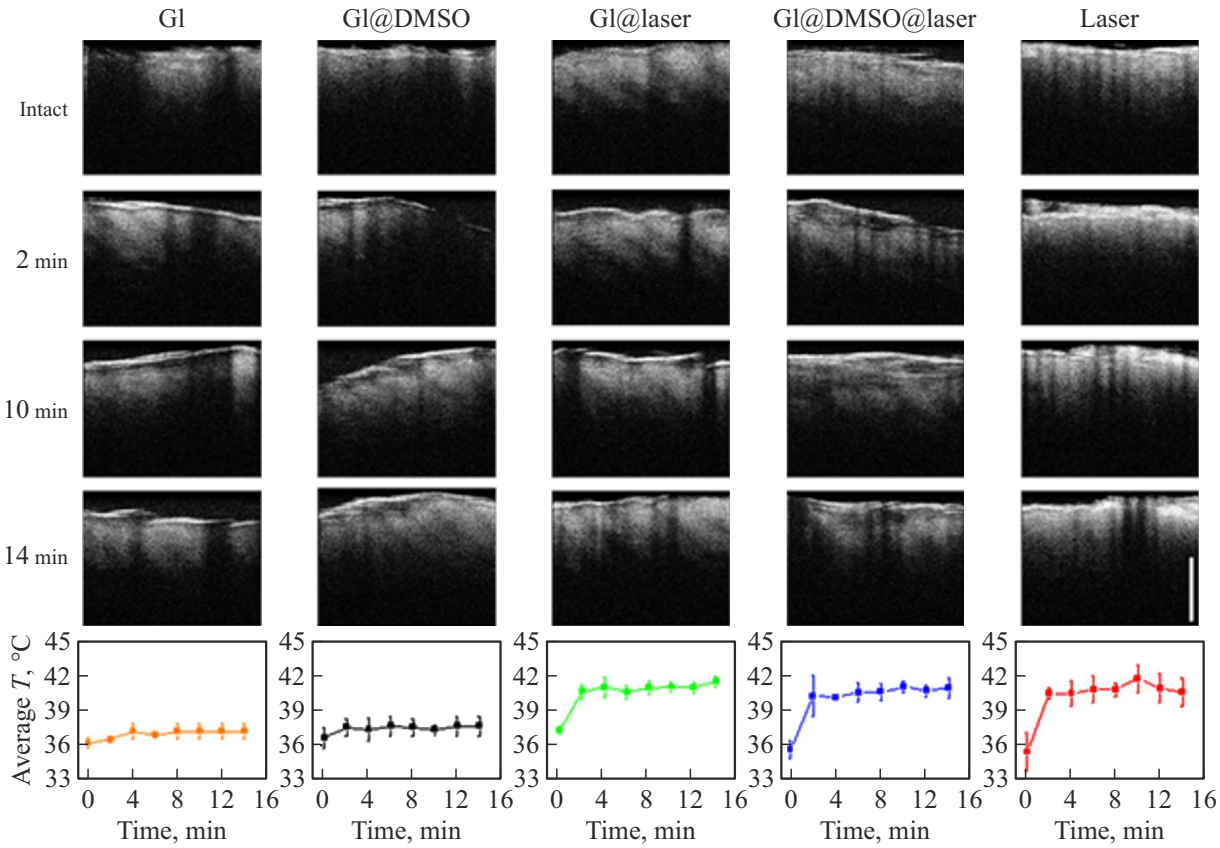

Figure 3. OCT images of rats skin sections *in vivo* after exposure of (*a*) glycerol water solution (Gl) and (*b*) mixture of 70% glycerol solution and 10% DMSO (Gl@DMSO) at body temperature, (*c*) 70% glycerol solution (Gl@laser) and (*d*) mixture of 70% glycerol solution and 10% DMSO (Gl@DMSO@laser) at laser heating and (*e*) laser heating (Laser). Scale bar corresponds to 500 μm. Dark vertical stripes on images are artefacts, appearing during animals breathing. Time variations of the average skin temperature value in place of exposure for various groups are presented under the corresponding OCT images.

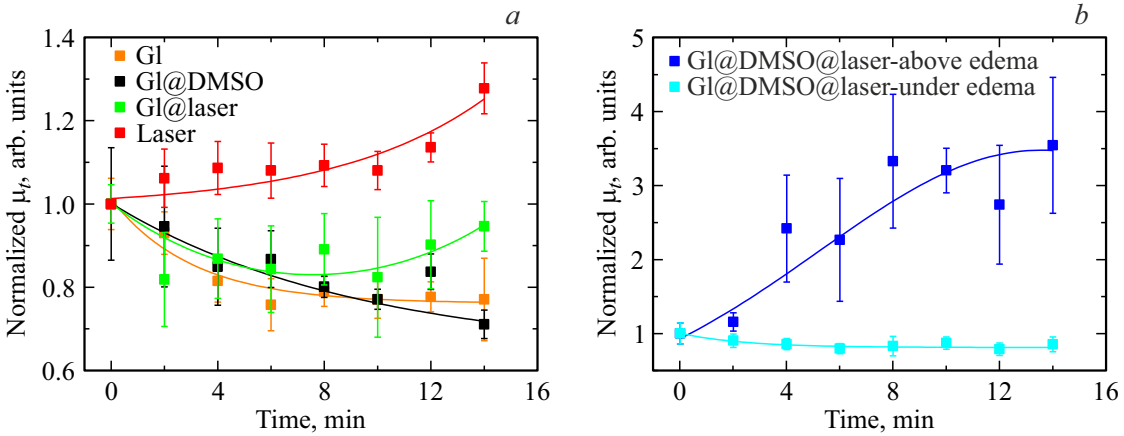

Figure 4. Time dependences of the averaged and normalized light attenuation coefficient in the examined groups: (*a*) I (Gl), II (Gl@DMSO), III (Gl@laser) and V (Laser) and (*b*) IV above edema area (Gl@DMSO@laser above edema) and under edema area (Gl@DMSO@laser under edema).

area under the edema continues to clear up, and μ_t value decreases by $20 \pm 8\%$ in average (fig. 4, *b*). This effect is probably related to DMSO action. It is known, that at high concentrations DMSO can result in skin irritation, accompanied with epidermal spongiosis [39]. In this case the edema appearance is stimulated by temperature increase to 41°C, while at temperature of 38°C there was no edema.

Fig. 3, *e* shows the significant brightness increase of tissue surface image, that indicates its induration, probably due to dehydration under laser heating exposure. Increase of attenuation coefficient as time passes is also seen in fig. 4, *a*, it was $28 \pm 6\%$ in average.

For the further studies Gl@DMSO was selected as OCA, since, despite the edema appearance, it results in the biggest reduction of the light attenuation coefficient in the skin.

Stages of pilot experiment with PPTT of model tumor of cholangiocarcinoma PC-1 with preliminary skin clearing, time dependences of skin heating temperature and diffuse reflection spectra of the skin above tumor, doped with GNR, before exposure, after 10 min of application of Gl@DMSO@laser and after 15 min of PPTT are presented in fig. 5. It is seen well in fig. 5, *a*, that erythema and skin edema are observed after Gl@DMSO@laser in the place of irradiation, that results in change of diffuse reflection spectra: reflection coefficient reduction in hemoglobin (543 and 577 nm) and water (1434 and 1958 nm) absorption bands (fig. 5, *c, d*). The observed differences in the registered valued of diffuse reflection at long-wavelength limit of the range of 420–1000 nm and short-wavelength limit of the range of 930–2125 nm are explained with the use of different spectrometers for measurements (see section Methods and materials) with different sensitivity in this wavelength range. However, the mutual position of diffusive reflection spectra of skin under exposure of the examined stimuli is in good agreement in both examined spectral bands. Fig. 5, *b* shows that at the similar mode of Gl@DMSO@laser, unlike rats without tumor (fig. 3, *d*), rat with tumor, doped with GNR, has a temperature increase from 41.5°C, 30 s after irradiation start, to 46.5°C, 10 min after, that probably is related to additional influence of nanoparticles heating in tumor body. Differences between the dependences of heating temperature on time for PPTT with preliminary clearing and without it were insignificant and can be related to different local content of nanoparticles in the irradiation area. At the same time there are significant changes in diffuse reflection spectrum in hemoglobin (transition from oxygenated HbO_2 to deoxygenated form of Hb and partial destruction of hemoglobin) and water (absorption bands shift towards more shortwave spectral region) absorption bands. Thus, for hemoglobin absorption bands (fig. 5, *c*) the transition of Q-bands from 543 and 577 nm to a single band at 561 nm at PPTT after Gl@DMSO@laser is observed, that is specific for hemoglobin deoxygenation [40]. At PPTT without preliminary exposure the disappearance of characteristic absorption bands of hemoglobin Hb and HbO_2 is observed in this spectral region, that can be related to protein coagulation, that occurs at blood hemoglobin heating [41]. Significant darkening and increase of affected region on a section, subject to PPTT, is seen in fig. 5, *a*. Water absorption bands at 1434 and 1958 nm for intact skin are shifted towards 1429 and 1934 nm at heating with Gl@DMSO@laser, towards 1420 and 1929 nm at PPTT after Gl@DMSO@laser and towards 1415 and 1922 nm at PPTT without preliminary exposure (fig. 5, *d*).

Beside changes of skin absorption properties, the changes of its scattering characteristics also influenced on the reflection spectra. Thus, the skin edema was observed under exposure of Gl@DMSO@laser, resulting in reflection coefficient reduction. At PPTT the more intense laser radiation resulted in tissue dehydration, its induration and, as a consequence, the reflection coefficient increase. It is interesting, that the preliminary application of OCA lowered the level of skin damage and prevented from permanent consequences of high temperature exposure on tissues, resulting in less significant changes of reflection spectra at PPTT with clearing than at PPTT.

Spectral dependences of optical parameters of the examined tumor tissues of a control animal (without introduction of GNR and irradiation), at PPTT with preliminary OCA application and heating and at PPTT without additional exposure are presented in fig. 6. The characteristics bands of HbO_2 (416–417, 544–548 and 566–574 nm, fig. 6, *a, b* and *d*) and water (1192, 1458 and 1942 nm) are seen in absorption spectra of the examined control animal tissues. Absorption bands of Hb (420 and 552 nm, fig. 6, *c*) are observed in the upper tumor part spectrum, that can be related to deoxygenation and start of the tissue necrotic changes.

In the absorption spectrum of the skin after PPTT procedure in fig. 6, *a* (sample 1, fig. 1) the increase of hemoglobin absorption bands and transition of HbO_2 into Hb are visible, indicating the vessels damage at PPTT. Besides, there are almost no water absorption bands in the spectrum of the skin after PPTT, that indicates the significant dehydration of the skin in the place of irradiation. In the spectrum of the skin after PPTT with preliminary clearing there are water absorption peaks, but they are shifted from 1192 and 1456 nm towards shorter wave lengths to 1188 and 1428 nm due to tissue heating. This shift is the most evident for sample of the skin above tumor, compared to other examined bio-tissues.

Damage of subdermal connective tissue (sample 2, fig. 1) after PPTT with clearing is also less evident than at PPTT, since the characteristic oxyhemoglobin bands (416, 548 and 574 nm) are present in the absorption spectrum.

GNR absorption peak (790 nm) is visible in tumor absorption and scattering spectra (fig. 6, *c, d*, samples 3 and 4, fig. 1) Maximum absorption shift relating to suspension maximum absorbance (800 nm) is explained, probably, with the influence of tissue scattering. Since absorption in the region of 790 nm is higher for the animal after PPTT, its local concentration of nanoparticles is higher. This can be explained by the fact, that as a result of GNR heating, the stronger tissue dehydration occurs in the tumor body after PPTT, resulting in more significant reduction of μ_a value on water absorption bands and maximum absorption shift towards the region of the shorter wave lengths.

Transport scattering coefficient reduces with a wave length increase, while the steeper slope of the spectrum corresponds to the higher temperature values in each layer. Increase of μ_s values in samples of skin and subdermal

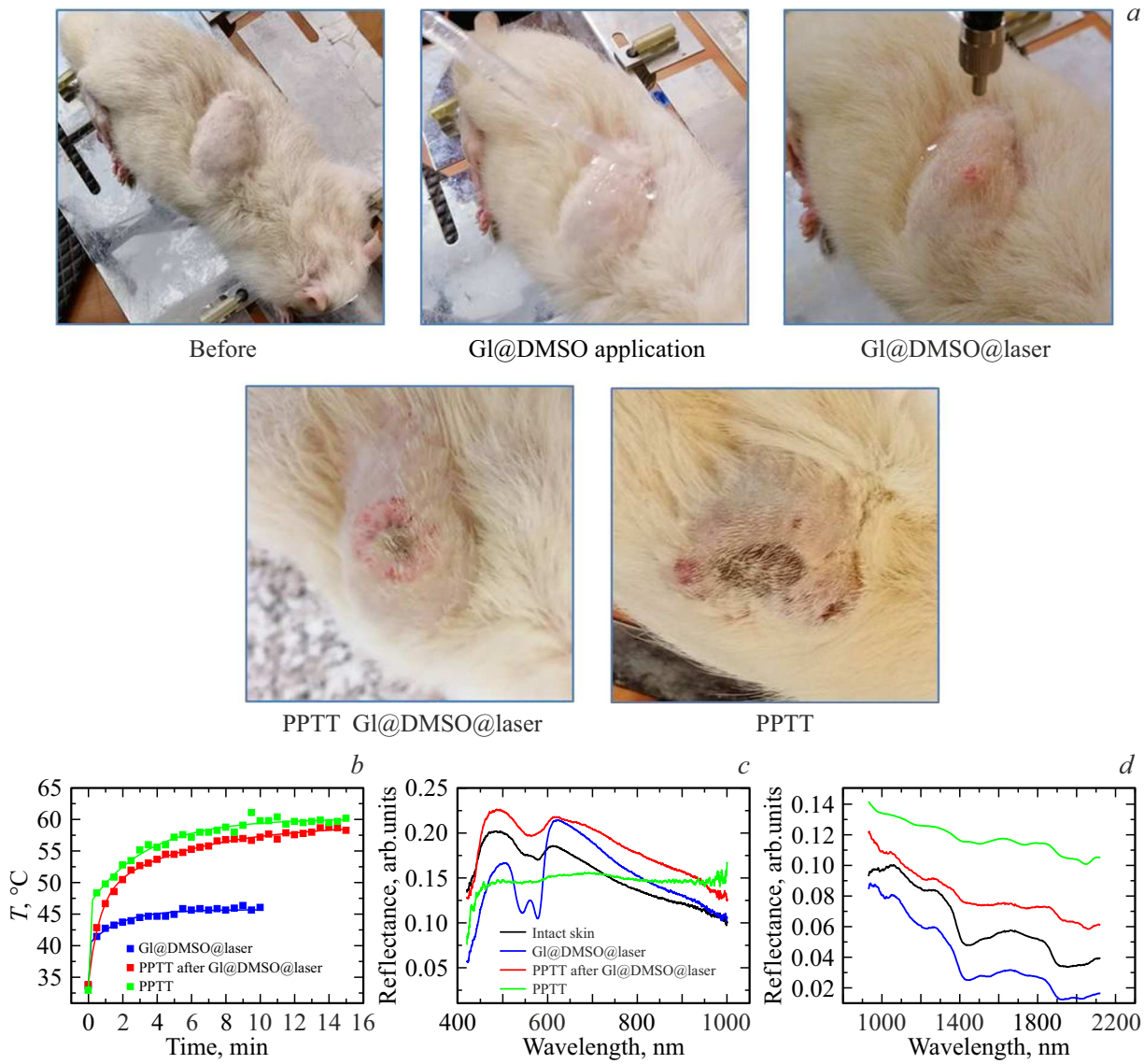

Figure 5. Picture of a rat *in vivo* with the implanted tumor PC-1, doped with GNR, showing the operational sequence and result of PPTT with preliminary skin clearing (*a*): before the procedure (Before), OCA application process (Gl@DMSO application), result of the low-intensity laser irradiation for 10 min (Gl@DMSO@laser) and with intensity increase for 15 min (PPTT after Gl@DMSO@laser) and additional image of tumor after PPTT without preliminary skin clearing (PPTT). Time dependences of the rat skin surface temperature during these procedures (*b*). Diffuse reflection spectra, measured before exposure and immediately after in spectral bands of (*c*) 420−1000 nm and (*d*) 930−2125 nm.

tissue after PPTT is explained with tissues coagulation, that results in destruction of larger scatterers, such as red blood cells, as well as walls of blood vessels and collagenic beams in skin and connective tissue. Protein coagulation also occurs in tumor body, especially in the area of contact with GNR.

The obtained results agree well with the literature data. Halldorsson [29] observed the higher optical absorption in thermally denaturated blood compared to native oxygenated blood at 633 and 1064 nm. Transformation between HbO_2 and Hb was quantitatively analyzed by Jia et al. [30]. Continuous heating at water bath to temperature of 60°C resulted in HbO_2 transformation into Hb. Effect of thermal changes in water absorption spectra was observed at direct measurements of water samples and laser therapy studies. Jansen et al. [42] showed that water absorption peak of about 1.94 μm shifted towards shorter wave lengths with temperature increase and reached 1.92 μm at 49°C. Blue shift of water absorption peaks at temperature increase was presented in the works [43–45]. The obtained results also agree well with the data from the works [27,28], where changes of optical parameters of skin at heating were reported. Small differences of values, specified in the literature, are probably caused by differences of the experimental conditions, theoretical models and tissue processing methods, used in the studies.

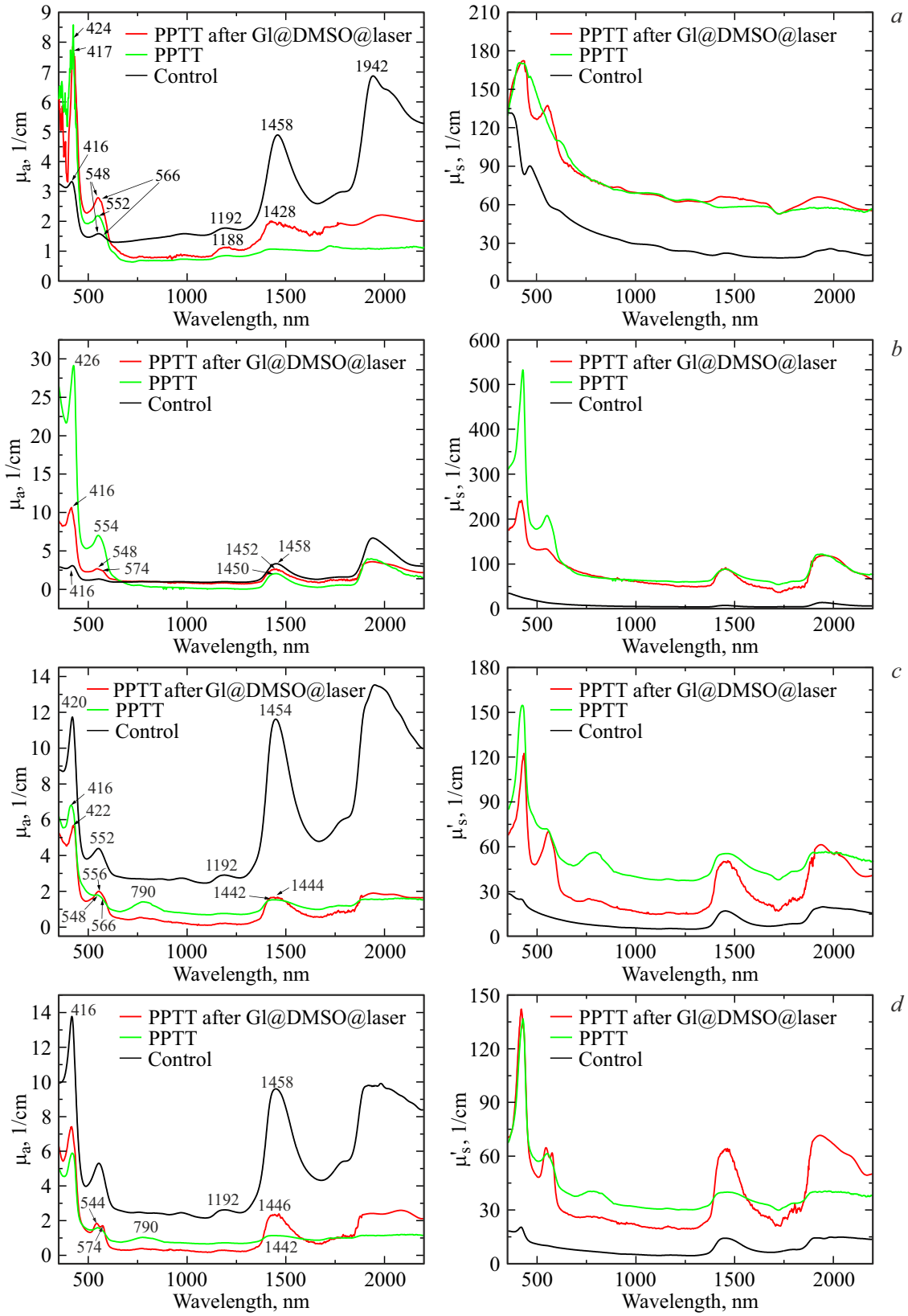

Figure 6. Absorption coefficient (μ_a) and transport scattering coefficient (μ_s') of tissues of control tumor, that was not subject to PPTT procedure (Control), tumor after PPTT with preliminary clearing (PPTT after Gl@DMSO@laser) and PPTT without preliminary clearing (PPTT): (*a*) skin above tumor, (*b*) subdermal connective tissue, (c) upper part of tumor and (*d*) lower part of tumor.

Based on data, presented in fig. 6, *c, d*, it is fair to assume that tumor body heating at PPTT without preliminary clearing (PPTT) was probably more significant, than at PPTT with preliminary clearing (PPTT after Gl@DMSO@laser), due to higher local concentration of particles in the place of irradiation. However, due to optical clearing of the surface the heating temperature at both procedures was comparable, thus allowed to achieve the close results. Computer simulation of the light propagation in tumor at preliminary optical clearing of the skin confirms this assumption.

Conclusion

In this work the changes of optical properties of the upper and lower parts of the model tumor of the rats (cholangiocarcinoma PC-1), skin and subdermal connective tissue, located above tumor, caused by temperature increase during PPTT procedure with preliminary optical clearing of the skin in the spectral band of 350−2200 nm, are presented for the first time. The results show, that the main differences of absorption are caused by blood deoxygenation, intratissual water heating and tissues dehydration in the area of irradiation, while the differences of scattering are caused by the destruction of micro-vessels with the following protein coagulation. Reduction of thermal skin damage as a result of PPTT at preliminary optical clearing with application of immersion agent and low-intensity laser irradiation is noted.

The results of this study can be used as a basis for refinement of PPTT models and procedure efficiency improvement by means of optical clearing of the skin.

Funding

The work was supported by the Russian Foundation for Basic Research grants № 19-32-90224 (in terms of PPTT method development) and № 20-52-56005 (in terms of malignant neoplasms optical parameters determination), and by the Innovation Promotion Fund grant UMNIK-19 (g)/Healthnet-NTI — 2019 № 15929GU/2020 dated 07.23.2020 (code 0059878, application U-65096).

Conflict of interest

The authors declare that they have no conflict of interest.

Compliance with ethical standards

The experiments were performed in accordance with the international ethical norms of the European Convention for the protection of vertebrate animals used for experimental and other scientific purposes (Strasbourg, 1986) and with recommendations of the Ethics Committee of the Federal State-Owned Publicly-Funded Institution of Higher Education Saratov State Medical University named after V.I. Razumovsky of the Ministry of Health of the Russian Federation (protocol № 6 dated 06.02.2018).

References

[1] J.R. Melamed, R.S. Edelstein, E.S. Day. ACS Nano, **9** (1), 6 (2015). DOI: 10.1021/acsnano.5b00021
[2] H.S. Jung, P. Verwilst, A. Sharma, J. Shin, J.L. Sessler, J.S. Kim. Chem. Soc. Rev., **47** (7), 2280 (2018). DOI: 10.1039/c7cs00522a
[3] X.-Q. Xu, Y. He, Y. Wang. Cell Rep. Phys. Sci., **2** (5), 100433 (2021). DOI: 10.1016/j.xcrp.2021.100433
[4] X. Huang, P.K. Jain, I.H. El-Sayed, M.A. El-Sayed. Lasers Med. Sci., **23** (3), 217 (2008). DOI: 10.1007/s10103-007-0470-x
[5] N.S. Abadeer, C.J. Murphy. J. Phys. Chem., **120** (9), 4691 (2016). DOI: 10.1021/acs.jpcc.5b11232
[6] Y. Liu, P. Bhattarai, Z. Dai, X. Chen. Chem. Soc. Rev., **48** (7), 2053 (2019). DOI: 10.1039/c8cs00618k
[7] M.M. Arnida, A. Janát-Amsbury, C.M. Ray, C.M. Peterson, H. Ghandehari. Eur. J. Pharm. Biopharm., **77** (3), 417 (2011). DOI: 10.1016/j.ejpb.2010.11.010
[8] L.M. Maestro, E. Camarillo, J.A. Sanchez-Gil, R. Rodriguez-Oliveros, J. Ramiro-Bargueno, A.J. Caamano, F. Jaque, J.G. Solea, D. Jaque. RSC Adv., **4** (96), 54122 (2014). DOI: 10.1039/C4RA08956A
[9] A.B. Bucharskaya, G.N. Maslyakova, M.L. Chekhonatskaya, G.S. Terentyuk, N.A. Navolokin, B.N. Khlebtsov, N.G. Khlebtsov, A.N. Bashkatov, E.A. Genina, V.V. Tuchin. Lasers Surg. Med., **50** (10), 1025 (2018). DOI: 10.1002/lsm.23001
[10] A.N. Bashkatov, K.V. Berezin, K.N. Dvoretskiy, M.L. Chernavina, E.A. Genina, V.D. Genin, V.I. Kochubey, E.N. Lazareva, A.B. Pravdin, M.E. Shvachkina, P.A. Timoshina, D.K. Tuchina, D.D. Yakovlev, D.A. Yakovlev, I.Yu. Yanina, O.S. Zhernovaya, V.V. Tuchin. J. Biomed. Opt., **23** (9), 091416 (2018). DOI: 10.1117/1.JBO.23.9.091416
[11] J.-I. Youn. Med. Laser, **10** (3), 146 (2021). DOI: 10.25289/ML.2021.10.3.146
[12] V.V. Tuchin. J. Phys. D Appl. Phys., **38** (15), 2497 (2005). DOI: 10.1088/0022-3727/38/15/001
[13] D. Zhu, J. Wang, Z. Zhi, X. Wen, Q. Luo. J. Biomed. Opt., **15**, 1 (2010). DOI: 10.1117/1.3369739
[14] R. Shi, L. Guo, C. Zhang, W. Feng, P. Li, Z. Ding, D. Zhu. J. Biophotonics., **10** (6−7), 887 (2017). DOI: 10.1002/jbio.201600221
[15] D.K. Tuchina, P.A. Timoshina, V.V. Tuchin, A.N. Bashkatov, E.A. Genina. IEEE J. Sel. Top. Quantum Electron., **25** (1), 7200508 (2019). DOI: 10.1109/JSTQE.2018.2830500
[16] X. Wen, Z. Mao, Z. Han, V.V. Tuchin, D. Zhu. J. Biophotonics, **3** (1−2), 44 (2010). DOI: 10.1002/jbio.200910080
[17] V.D. Genin, E.A. Genina, V.V. Tuchin, A.N. Bashkatov. J. Innov. Opt. Health Sci., **14** (5), 2142006 (2021). DOI: 10.1142/S1793545821420062
[18] D.K. Tuchina, V.D. Genin, A.N. Bashkatov, E.A. Genina, V.V. Tuchin. Opt. Spectr., **120** (1), 28 (2016). DOI: 10.1134/S0030400X16010215.
[19] J. Wang, N. Ma, R. Shi, Y. Zhang, T. Yu, D. Zhu. IEEE J. Sel. Top. Quantum Electron., **20** (2), 7101007 (2014). DOI: 10.1109/JSTQE.2013.2289966
[20] J. Jiang, R.K. Wang. Phys. Med. Biol., **49** (23), 5283 (2004). DOI: 10.1088/0031-9155/49/23/006
[21] J. Jiang, M. Boese, P. Turner, R.K. Wang. J. Biomed. Opt., **13** (2), 0211052008 (2008). DOI: 10.1117/1.2899153
[22] E.A. Genina, A.N. Bashkatov, E.A. Kolesnikova, M.V. Basco, G.S. Terentyuk, V.V. Tuchin. J. Biomed. Opt., **19** (2), 021109 (2014). DOI: 10.1117/1.JBO.19.2.021109

[23] O. Stumpp, A.J. Welch, J. Neev. Lasers Surg. Med., **37** (4), 278 (2005). DOI: 10.1002/lsm.20237
[24] C. Liu, Z. Zhi, V.V. Tuchin, Q. Luo, D. Zhu. Lasers Surg. Med., **42** (2), 132 (2010). DOI: 10.1002/lsm.20900
[25] G. Terentyuk, E. Panfilova, V. Khanadeev, D. Chumakov, E. Genina, A. Bashkatov, V. Tuchin, N. Khlebtsov, B. Khlebtsov. Nanoresearch, **7** (3), 325 (2014). DOI: 10.1007/s12274-013-0398-3
[26] Y. Chu, Sh. Liao, H. Liao, Y. Lu, X. Geng, D. Wu, J. Pei, Y. Wang. CCS Chem., **3**, 3289 (2021). DOI: 10.31635/ccschem.021.202101539
[27] J. Laufer, R. Simpson, M. Kohl, M. Essenpreis, M. Cope. Phys. Med. Biol., **43** (9), 2479 (1998). DOI: 10.1088/0031-9155/43/9/004
[28] T.W. Iorizzo, P.R. Jermain, E. Salomatina, A. Muzikansky, A.N. Yaroslavsky. Sci. Rep., **11** (1), 754 (2021). DOI: 10.1038/s41598-020-80254-9
[29] T. Halldorsson. In: Proc. 4thCongr. Int. Soc. Laser. Surgery (1981), p. 1–8.
[30] H. Jia, B. Chen, D. Li. Lasers Med. Sci., **32** (3), 513 (2017). DOI: 10.1007/s10103-017-2143-8
[31] N. Manuchehrabadi, Y. Chen, A. LeBrun, R. Ma, L. Zhu. J. Biomech. Eng., **135** (12), 121007 (2013). DOI: 10.1115/1.4025388
[32] V.D. Genin, E.A. Genina, A.B. Bucharskaya, M.L. Chekhonatskaya, G.S. Terentyuk, D.K. Tuchina, N.G. Khlebtsov, V.V. Tuchin, A.N. Bashkatov. J. Biomed. Photon. & Eng., **4** (1), 010505 (2018). DOI: 10.18287/JBPE18.04.010505
[33] H. Xie, B. Goins, A. Bao, Z.J. Wang, W.T. Philips. Int. J. Nanomed., **7**, 2227 (2012). DOI: 10.2147/IJN.S30699
[34] R.K. Wang, V.V. Tuchin. Optical coherence tomography. Light scattering and imaging enhancement, ed. by V.V. Tuchin (Springer, New York, Heidelberg, Dordrecht, London, 2013), p. 665–742. DOI: 10.1007/978-1-4614-5176-1_16
[35] D.J. Faber, F.J. van der Meer, M.C.G. Aalders, T.G. van Leeuwen. Opt. Express, **12** (19), 4353 (2004). DOI: 10.1364/OPEX.12.004353
[36] E.A. Genina, N.S. Ksenofontova, A.N. Bashkatov, G.S. Terentyuk, V.V. Tuchin. Quant. Electr., **47** (6), 561 (2017). DOI: 10.1070/QEL16378
[37] S.A. Prahl, M.J.C. van Gemert, A.J. Welch. Appl. Opt., **32** (4), 559 (1993). DOI: 10.1364/AO.32.000559
[38] A.N. Bashkatov, E.A. Genina, M.D. Kozintseva, V.I. Kochubei, S.Yu. Gorodkov, V.V. Tuchin. Opt. Spectr., **120** (1), 1 (2016). DOI: 10.1134/S0030400X16010045
[39] A. Pagnoni, A. Knuettel, P. Welker, M. Rist, T. Stoudemayer, L. Kolbe, I. Sadiq, A.M. Kligman. Skin Res. Technol., **5** (2), 83 (1999). DOI: 10.1111/j.1600-0846.1999.tb00120.x
[40] S.A. Prahl. Optical absorption of haemoglobin [Electronic source]. URL: http://www.omlc.ogi.edu/spectra/
[41] J.K. Barton, G. Frangineas, H. Pummer, J.F. Black. Photochem. Photobiol., **73** (6), 642 (2001). DOI: 10.1562/0031-8655(2001)073¡0642:cpitpt¿2.0.co;2
[42] E.D. Jansen, T.V. van Leeuwen, M. Motamedi, C. Borst, A. Welch. Laser Surg. Med., **14** (3), 258 (1994). DOI: 10.1002/lsm.1900140308
[43] V.S. Langford, A.J. McKinley, T.I. Quickenden. J. Phys. Chem. A., **105** (39), 8916 (2001). DOI: 10.1021/JP010093M
[44] B.I. Lange, T. Brendel, G. Huttmann. Appl. Opt., **41** (27), 5797 (2002). DOI: 10.1364/ao.41.005797
[45] E.H. Otal, F.A. Icyn, F.J. Andrade. Appl. Spectrosc., **57** (6), 661 (2003). DOI: 10.1366/000370203322005355